Resonant Oscillation of Misch-Metal Atoms in Filled Skutterudites

Yaguo Wang,[1] Xianfan Xu,[1,*] and Jihui Yang[2,†]

[1]*School of Mechanical Engineering and Birck Nanotechnology Center, Purdue University, West Lafayette, Indiana 47907, USA*
[2]*Materials and Processes Lab, GM R&D Center, Warren, Michigan 48090, USA*

(Received 20 December 2008; published 1 May 2009)

We investigate vibrational behaviors in misch-metal filled antimony skutterudites in the time domain. At higher filling ratios of guest atoms, the vibration frequency approaches that of the cage structure and the amplitude becomes stronger. Furthermore, the reduction of lattice thermal conductivity over a wide temperature range can be explained using the measured resonant vibrational frequency. These findings reveal that the reduction of the lattice thermal conductivity is a result of scattering of acoustic phonons due to the resonant interaction between guest atoms and lattice phonons.

DOI: 10.1103/PhysRevLett.102.175508 PACS numbers: 63.20.−e, 65.40.−b, 78.47.J−

Caged compounds such as skutterudites and clathrates filled with guest atoms are found to have a significantly reduced thermal conductivity [1,2], favorable for being used as thermoelectric materials. A concept called ''phonon-glass-electron-crystal (PGEC)'' was used to describe the role of guest atoms in the cages constructed by host atoms [3]. The guest atoms are weakly bonded to the cage structure and vibrate locally and incoherently, hence the name ''rattler''. These rattlers provide an extra phonon-scattering channel and decrease the phonon mean free path, which results in the suppression of the lattice thermal conductivity [4]. Vigorous efforts have been directed toward revealing the vibrational properties of filled skutterudites. Infrared (IR) absorption spectroscopy [5] and Raman spectroscopy [6,7] were used to identify IR and Raman active modes. Rattling of guest atoms, on the other hand, was not observed in Raman spectroscopy, consistent with first-principles calculations that showed rattling is not Raman active [8]. Inelastic neutron scattering [9,10] and nuclear inelastic scattering [11] were used to determine the low-energy localized vibration modes of the rattlers. The PGEC paradigm was challenged in two recent studies [12,13]. Neutron spectroscopy and *ab initio* computations of La- and Ce-filled Fe_4Sb_{12} skutterudites showed well-defined phase relations and quasiharmonic coupling between the guests and the host lattice, and the phonon crystal behavior of the host [12]. In another neutron triple-axis spectroscopy study, the guest atoms in a clathrate material were found to lower the velocity of acoustic phonons [13]. Therefore, it is still an open question regarding the role of guest atoms.

Here we carry out ultrafast time-resolved optical measurements to investigate vibrational behaviors of filled antimony skutterudites. Ultrafast time-resolved optical measurement is a powerful tool to detect vibrational modes [14,15] and has been used recently to investigate phonon vibrations and scattering in Bi and Bi_2Te_3/Sb_2Te_3 superlattice materials [16,17]. In this work, the ultrafast optical measurement is used to elucidate interactions between guest atoms and the host lattice in misch-metal filled antimony skutterudites. For the first time, vibrations caused by guest atoms is observed in the time domain. The results reveal strong interactions between guest atoms and the host lattice that reduce lattice thermal conductivity.

Samples were prepared using procedures documented in other publications [18]. The filling materials are misch metal noted by Mm. The starting misch metal consists of Ce, La, Nd, Pr, Si, Fe, Al and O with atomic percentages of 50.75, 22.75, 16.22, 5.72, 3.35, 0.72, 0.50, and less than 0.01, respectively, which were determined using Electron Probe Microanalysis (EPMA) with an uncertainty less than 2%. The use of misch metal instead of pure rare-earth elements was mainly due to its much lower cost and therefore its potentials for being used in commercial products. It is noted that the four primary rare-earth elements in the misch metal, Ce, La, Nd, and Pr, consist of 95.44% of the total material whereas their atomic weights vary from 138.9 to 144.2 only. Therefore, it is expected that the misch metal would have similar effect as those pure rare-earth elements. Five samples are studied in this work, including one unfilled skutterudite sample. Their compositions, determined by EPMA, and corresponding nominal representations are listed in Table I. X-ray powder diffraction was performed on a Philips diffractometer and the data indicate all samples are phase pure with the exception of trace amounts of Sb, $FeSb_2$ and $MmSb_2$ ($\leq$1 vol%).

TABLE I. Nominal representations and compositions of filled and unfilled skutterudites.

Nominal representation	Composition
$Co_{0.9}$ (unfilled)	$Co_{0.9}Fe_{0.1}Sb_3$
$Mm_{0.55}$	$Mm_{0.55}Fe_{2.44}Co_{1.56}Sb_{11.96}$
$Mm_{0.65}$	$Mm_{0.65}Fe_{2.92}Co_{1.08}Sb_{11.98}$
$Mm_{0.72}$	$Mm_{0.72}Fe_{3.43}Co_{0.57}Sb_{11.97}$
$Mm_{0.82}$	$Mm_{0.82}Fe_4Sb_{11.96}$

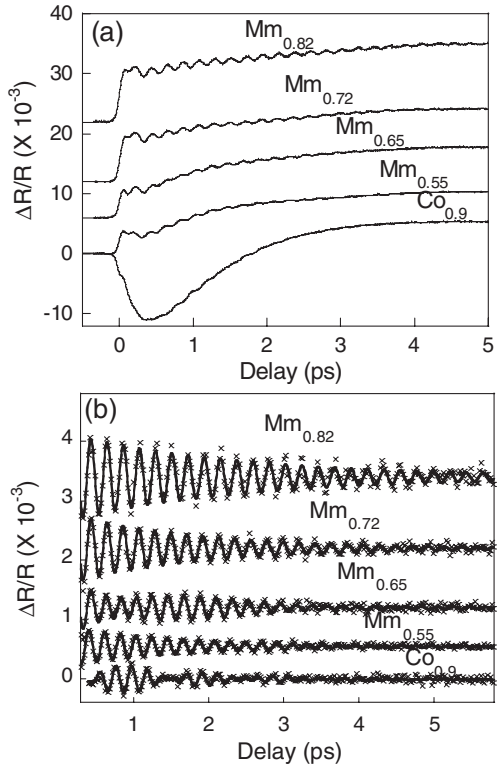

FIG. 1. Time-resolved reflectivity of unfilled and filled samples. (a) The as-recorded data. The oscillations are due to the host lattice in the unfilled skutterudite or interactions between the guest atoms and host lattice in the filled skutterudites (see text). (b) Oscillatory signals after the carrier signals are removed. The "x" symbols are experimental data points, and the lines are fitting results. In both (a) and (b), data are shifted along the vertical axis for clarity.

Ultrafast optical measurements are performed in a collinear pump-probe scheme. Laser pulses with 50 fs FWHM (full width at half maximum) are generated by a Spectra Physics Ti:sapphire system with the center wavelength at 800 nm and a repetition rate of 1 kHz. A second harmonic crystal is used to generate pump pulses centered at 400 nm. The pump and probe beams are focused onto the sample at normal direction with diameters of 80 and 20 μm and fluences of 2.2 mJ/cm^2 and 0.02 mJ/cm^2, respectively. The pump beam is modulated by a chopper and the reflected probe beam is measured. The time resolution is about 7 fs.

Time-resolved reflectivity data of all the samples are shown in Fig. 1. The difference in the immediate responses in the filled and unfilled samples is due to the change to the electronic structure and its excitation state by filling, and the nature of this change will be investigated in another study. Figure 1(b) shows the oscillation signals after removing the background nonoscillatory part using a digital filter. The dominant oscillation frequencies can be determined by fitting the experimental data with a damping harmonic oscillator model [17,19], and the fitted frequencies are listed in Table II. For the filled skutterudites, the uncertainty in frequency determination is about ± 0.02 THz. The damping and revival behavior of oscillation in $Mm_{0.65}$ indicates the existence of two vibrational modes, and two oscillators are used to fit the data. For the unfilled sample, the oscillation is weaker and only the first few oscillations were used, and the vibration frequency is found to be about 4.6 THz with an uncertainty of ± 0.2 THz.

TABLE II. Frequencies of oscillation in unfilled and filled skutterudites.

Sample	$Co_{0.9}$	$Mm_{0.55}$	$Mm_{0.65}$	$Mm_{0.72}$	$Mm_{0.82}$
Ω (THz)	4.6	4.82	4.76, 4.42	4.69	4.62

An important finding from Fig. 1(b) is that the vibrational amplitude increases with increasing filling ratio, indicating the effect of filling on the vibration of the guest-host system. To identify these strong oscillations, the Stokes Raman spectra are also collected on the same samples using a Jobin Yvon T64000 Raman system with a 514.5 nm excitation source and a spectral resolution better than 1 cm^{-1}. It can be seen from Fig. 2 that, whereas the Raman measurements detect the A_g optical phonon modes in the host lattice, the modes measured with ultrafast optical experiments are in general different from the Raman modes. The two dashed lines in Fig. 2 shows the two A_g modes of the Sb_4 ring [6], and the arrows are the frequencies obtained from the ultrafast optical measurements. Table II and Fig. 2 show that, with lower filling ratios, the differences between the Raman modes and the ultrafast pump-probe measured modes are larger. This is consistent with the theory that vibrations associated with

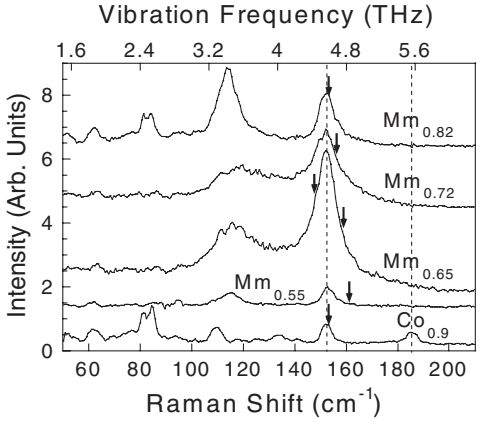

FIG. 2. Raman spectra. Vertical dashed lines mark the two A_g modes of the Sb_4 ring, and the arrows show the frequencies from ultrafast optical experiments. Data are shifted vertically for clarity. The vibration frequencies measured in the ultrafast measurement approach that of the host Sb4 ring at higher filling ratio, indicating stronger guest-host interactions at a higher filling ratio.

the filled atoms are not Raman active [8]. As the filling ratio increases, the vibration frequency approaches that of the lower-frequency A_g mode of the Sb_4 ring structure. This is because with a higher filling ratio, the interactions between guest atoms and the host lattice become stronger (the larger vibrational amplitude in the ultrafast optical measurement). This stronger interaction causes the vibration frequency to shift closer to that of the host lattice, which was predicted by Li *et al.* [7].

The collective motion of guest atoms and the host lattice is also similar to the results obtained in Koza *et al.*'s work, where the coherent coupling between guest atoms and the host lattice was detected even though their work was focused on lower energy modes [12]. Also as suggested by Keppens *et al.*, there exist two eigenmodes of filled atoms in $La_{0.9}Fe_3CoSb_{12}$ [9]: the more localized lower-frequency mode is associated with La moving towards the "void" and the higher frequency mode is the motion towards a nearest-neighboring Sb atom. The oscillations observed in ultrafast optical experiments are related to the higher frequency coupling between guest atoms and host Sb atoms.

To evaluate the effect of vibrational modes on lattice thermal conductivity, the measured vibration frequencies are used to compute lattice thermal conductivity using the resonance scattering model [20]. Thermal conductivity measurements were made in a Quantum Design physical property measurement system between 2 and 300 K. The electronic contributions to the conductivity were subtracted using the data from resistivity measurements and the Wiedemann-Franz Law. The accuracy of our thermal conductivity data is 10% near room temperature and averages about 5% over the measurement temperature range. According to the Debye theory, lattice thermal conductivity can be expressed as [21]:

$$\kappa_L = \frac{k_B}{2\pi^2 v}\left(\frac{k_B T}{\hbar}\right)^3 \int_0^{\theta_D/T} \frac{x^4 e^x}{\tau_C^{-1}(e^x - 1)^2}\, dx, \qquad (1)$$

where $x = \hbar\omega/k_B T$, $\hbar$ is the reduced Planck constant, ω the phonon frequency, k_B the Boltzmann constant, T the absolute temperature, v the sound velocity, θ_D the Debye temperature, and τ_C the phonon relaxation time which can be described as a summation of various phonon-scattering processes [18,20]:

$$\tau_C^{-1} = \frac{v}{L} + A\omega^4 + B\omega^2 T \exp\left(-\frac{\theta_D}{3T}\right) + \frac{C\omega^2}{(\Omega^2 - \omega^2)^2}, \qquad (2)$$

where L, A, B, and C represent grain-boundary, point defect, umklapp, and phonon resonant scattering, respectively. The last term, the phonon resonant scattering, is the resonant interaction between guest atoms and lattice phonons, with the resonant frequency Ω obtained from the ultrafast optical measurements. The Debye temperature θ_D used in the calculation is 270 K for all samples, which is determined from the temperature dependent specific heat measurement.

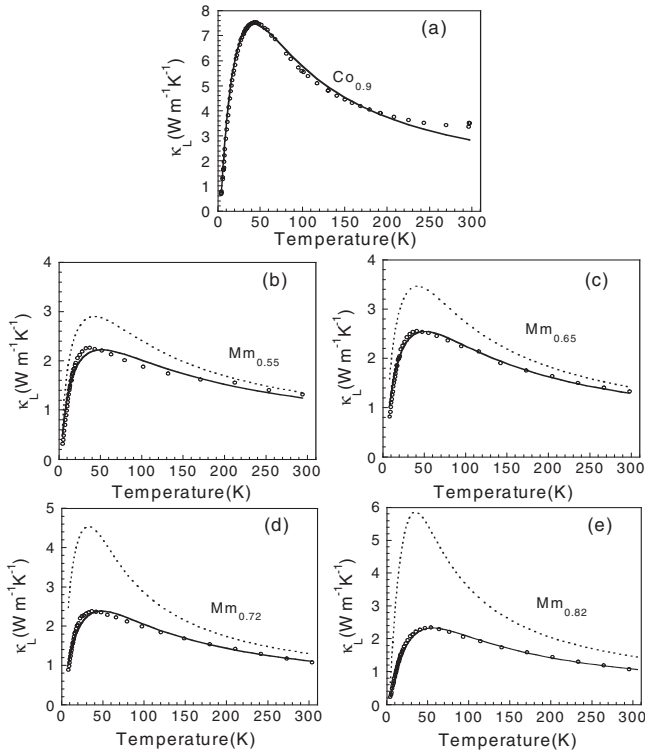

FIG. 3. Lattice thermal conductivities as a function of temperature. Circles are experimental data. Solid and dashed lines are calculation results with and without resonant scattering, respectively.

Figure 3 shows that lattice thermal conductivities of filled and unfilled samples can be modeled very well over the entire 2 orders of magnitude temperature span. The dashed lines in Figs. 3(b)–3(e) show lattice thermal conductivities without the resonant scattering term. It is clear that resonant scattering of phonons is effective in reducing lattice thermal conductivity. Table III lists the parameters used in computing the data in Fig. 3. The influence on lattice thermal conductivity from each parameter was discussed in a sensitivity study in a previous publication [18]. The fact that each parameter dominates a different temperature range allows for determining the fitting parameters relatively accurately. Here, based on $\pm 5\%$ experimental uncertainty of thermal conductivity data, the uncertainties of L, A, B, and C are estimated to

TABLE III. Parameters used in Eqs. (1) and (2).

Samples	L (μm)	A (10^{-43} s^3)	B (10^{-18} sK^{-1})	C (10^{38} s^{-3})
$Co_{0.9}$	3.03	84.754	5.951	0
$Mm_{0.55}$	4.35	404.88	6.712	1.736
$Mm_{0.65}$	3.15	267.707	8.66	1.851
$Mm_{0.72}$	7.21	244.562	11.461	2.897
$Mm_{0.82}$	2.37	96.667	16.07	4.988

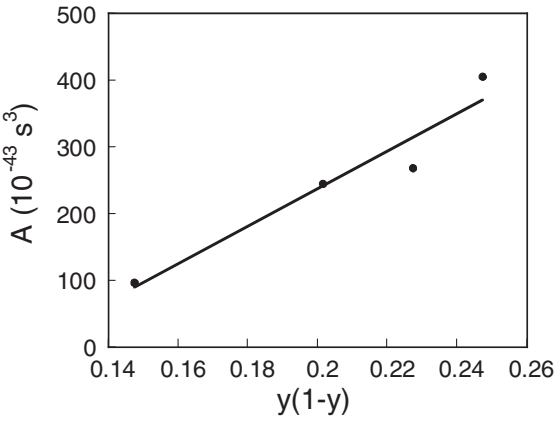

FIG. 4. Point defect scattering coefficient A vs $y(1\text{-}y)$, where y is the filling ratio.

be about $\pm 32\%$, $\pm 20\%$, $\pm 20\%$, and $\pm 10\%$, respectively. It is also noticed from Fig. 3 that thermal conductivity reductions in all filled samples are similar. This is because the resonant scattering causes more reduction in thermal conductivity in samples with higher filling ratio (Fig. 3), whereas scattering from point defect is maximum when the filling ratio is about 50%. Phonon-point defect scattering is mainly due to the mass fluctuation between filled atoms (y) and void ($1\text{-}y$) [22]. Figure 4 plots the point defect scattering parameter A against $y(1\text{-}y)$ and a linear dependence can be seen, which is consistent with [22].

Our results suggest that interactions between guest atoms and the host lattice reduce the lattice thermal conductivity. This is not exactly the same as the PGEC theory [1,3,4] that the rattling of guest atoms causes thermal conductivity reduction. Our results suggest, instead of guest atoms acting alone, the resonant interactions between guest atoms and the host lattice (the mode between the guest atoms and the neighboring Sb atoms described in [9]) causes additional scattering to the acoustic phonons and reduces lattice thermal conductivity.

In summary, we investigated vibrational behaviors of misch-metal filled antimony skutterudites in the time domain using ultrafast optical measurements. Our results revealed resonant interactions between guest atoms and the host lattice. The reduction of lattice thermal conductivities was explained with the measured vibration frequencies over a large temperature range, indicating that resonant interactions between guest atoms and the host lattice act as additional scattering centers of acoustic phonons and reduce lattice thermal conductivity.

We want to thank Dr. A. Q. Wu for his initiative and valuable efforts on this project, and Dr. V. Drachev for his help on Raman spectroscopy. Partial support to this work by the Sandia National Laboratory (No. 620550) and the Air Force Office of Scientific Research (FA9550-08-1-0091) are gratefully acknowledged. J. Y. wants to thanks Jan F. Herbst and Mark Verbrugge for continuous support and encouragement. The work is also in part supported by G.M. and by the Department of Energy under corporate agreement DE-FC26-04NT42278.

*To whom correspondence should be addressed. Phone: (765) 494-5639
xxu@ecn.purdue.edu
†jihui.yang@gm.com

[1] B. C. Sales, D. Mandrus, and R. K. Williams, Science **272**, 1325 (1996).
[2] K. A. Kovnir and A. V. Shevelkov, Russian Chemical Reviews **73**, 923 (2004).
[3] G. A. Slack, in *CRC Handbook of Thermoelectrics*, edited by D. M. Rowe (CRC Press, Boca Raton, 1995).
[4] G. S. Nolas, D. T. Morelli, and T. M. Tritt, Annu. Rev. Mater. Sci. **29**, 89 (1999).
[5] S. V. Dordevic *et al.*, Phys. Rev. B **60**, 11 321 (1999).
[6] G. S. Nolas *et al.*, J. Appl. Phys. **79**, 2622 (1996).
[7] L. X. Li *et al.*, Chem. Phys. Lett. **347**, 373 (2001).
[8] J. L. Feldman *et al.*, Phys. Rev. B **68**, 094301 (2003).
[9] V. Keppens *et al.*, Nature (London) **395**, 876 (1998).
[10] R. P. Hermann *et al.*, Phys. Rev. Lett. **90**, 135505 (2003).
[11] G. J. Long *et al.*, Phys. Rev. B **71**, 140302 (2005).
[12] M. M. Koza *et al.*, Nature Mater. **7**, 805 (2008).
[13] M. Christensen *et al.*, Nature Mater. **7**, 811 (2008).
[14] T. K. Cheng *et al.*, Appl. Phys. Lett. **57**, 1004 (1990).
[15] T. E. Stevens, J. Kuhl, and R. Merlin, Phys. Rev. B **65**, 144304 (2002).
[16] A. Q. Wu, X. Xu, and R. Venkatasubramanian, Appl. Phys. Lett. **92**, 011108 (2008).
[17] Y. Wang, X. Xu, and R. Venkatasubramanian, Appl. Phys. Lett. **93**, 113114 (2008).
[18] J. Yang *et al.*, Phys. Rev. B **67**, 165207 (2003).
[19] O. V. Misochko *et al.*, Phys. Rev. Lett. **92**, 197401 (2004).
[20] R. O. Pohl, Phys. Rev. Lett. **8**, 481 (1962).
[21] J. Callaway, Phys. Rev. **113**, 1046 (1959).
[22] G. P. Meisner *et al.*, Phys. Rev. Lett. **80**, 3551 (1998).